



[Gly14]-Humanin Protects Against Amyloid β Peptide-Induced Impairment of Spatial Learning and Memory in Rats

Li Yuan¹ · Xiao-Jie Liu² · Wei-Na Han³ · Qing-Shan Li¹ · Zhao-Jun Wang¹ · Mei-Na Wu¹ · Wei Yang¹ · Jin-Shun Qi¹

Received: 10 January 2016 / Accepted: 11 May 2016 / Published online: 15 June 2016

© Shanghai Institutes for Biological Sciences, CAS and Springer Science+Business Media Singapore 2016

Abstract Alzheimer disease (AD), a progressive neurodegenerative disorder, is characterized by cognitive decline and the accumulation of senile plaques in the brain. Amyloid β protein (A β) in the plaques is thought to be responsible for the memory loss in AD patients. [Gly14]-humanin (HNG), a derivative of humanin (HN), has much stronger neuroprotective effects than natural HN *in vitro*. However, clarification of the A β active center and the neuroprotective mechanism of HN still need *in vivo* evidence. The present study first compared the *in vivo* biological effects of three A β fragments (1–42, 31–35, and 35–31) on spatial memory in rats, and investigated the neuroprotective effects and molecular mechanisms of HNG. The results showed that intrahippocampal injection of A β_{1-42} and A β_{31-35} almost equally impaired spatial learning and memory, but the reversed sequence A β_{35-31} did not have any effect; a high dose of A β_{31-35} (20 nmol) produced a more detrimental response than a low dose (2 nmol); A β_{31-35} injection also disrupted gene and protein expression in the hippocampus, with up-regulation of caspase3 and down-regulation of STAT3; pretreatment with HNG not only protected spatial memory but also rescued STAT3 from A β -induced disruption; and the neuroprotective effects of HNG were effectively counteracted by genistein, a specific tyrosine kinase inhibitor. These results

clearly show that sequence 31–35 in A β is the shortest active center responsible for the neurotoxicity of A β from molecule to behavior; and HNG protects spatial learning and memory in rats against A β -induced insults; and probably involves the activation of tyrosine kinases and subsequent beneficial modulation of STAT3 and caspase3.

Keywords [Gly14]-humanin · Amyloid β peptide · Spatial learning and memory · STAT3 · Caspase 3

Introduction

Alzheimer disease (AD) is an insidious and progressive neurodegenerative disorder characterized by global cognitive decline and robust accumulation of senile plaques in the brain [1]. These hallmarks of AD are found most commonly in the hippocampus and neocortex, regions associated with memory [2]. The main component of senile plaques is amyloid β protein (A β), a 39–43 amino-acid peptide. The aggregation of A β oligomer is a key step in the pathogenic mechanism of AD; it triggers neuronal cell death and gradual cognitive decline [3, 4]. The neurotoxicity of the A β fragments A β_{1-42} , A β_{1-40} , and A β_{25-35} has been widely reported *in vivo* and *in vitro* [5–7]. In our previous experiments, we also found that A β_{31-35} , a shorter sequence than A β_{25-35} , mimics most of the neurotoxic effects of A β_{25-35} or full-length A β . For example, A β_{31-35} induces apoptosis in cultured cortical neurons [7] and PC12 cells [8], enhances intracellular Ca²⁺ loading by forming new ion channels [9], and suppresses delayed-rectifying K⁺ channels and BK channels in isolated hippocampal neurons [10]. Moreover, A β_{31-35} , like A β_{25-35} , has potent suppressive effects on hippocampal long-term potentiation (LTP) *in vivo* [7, 11] and *in vitro* [12]. Therefore, we set

✉ Jin-Shun Qi
jinshunqi2009@163.com

¹ Department of Physiology, Shanxi Medical University, Taiyuan 030001, China

² Department of Pharmacology and Toxicology, Medical College of Wisconsin, Milwaukee, WI 53226, USA

³ Department of Physiology, Shaoyang Medical College, Shaoyang 422000, China

out to further clarify whether A β_{31-35} and its inverse sequence A β_{35-31} impair the learning and memory behavior of rats, as has been reported for A β_{1-42} . So, we first compared the effects of three A β fragments (A β_{1-42} , A β_{31-35} , and A β_{35-31}) on spatial memory in rats. Then, we examined the neuroprotective action of [Gly14]-humanin (HNG) against A β and investigated its probable molecular mechanisms

Materials and Methods

Animals and Drugs

Adult male Sprague-Dawley rats (220–250 g) were obtained from the Research Animal Center of Shanxi Medical University, and all procedures were approved by the Shanxi Committee on Ethics in Animal Experiments. The rats were kept in a room with a controlled temperature (23 ± 2 °C, humidity (60%–80%), and lighting (12:12 h light-dark cycle). The compounds A β_{1-42} , A β_{31-35} , A β_{35-31} , HNG, and genistein were from Sigma (St. Louis, MO). All peptides were dissolved in saline except genistein (0.5% DMSO). The stock solutions were stored at -20 °C for A β or -80 °C for HNG. After 1 week of acclimatization, rats were anesthetized by intraperitoneal (*i.p.*) injection of 10% chloral hydrate (0.3 mL/100 g) and placed on a stereotaxic apparatus (Narishige, Tokyo, Japan) for acute surgery. Two small holes were drilled in the skull (3.0 mm posterior to bregma and 2.2 mm lateral to the midline) for bilateral intrahippocampal injection of drugs. Drugs were delivered into the bilateral hippocampal CA1 region in a total volume of 3 μ L within 5 min using a Hamilton microsyringe. In the co-application group, HNG was injected 5 min before A β_{31-35} .

Morris Water-Maze Test

Two weeks after operation and drug injection, the spatial learning and memory behavior of rats was evaluated using the Morris water-maze. The maze (Zhenghua Bio Instruments Ltd., Huaibei, China,) was a circular pool with a diameter of 150 cm and a wall height of 60 cm, made of stainless steel and painted flat black on the inner surface. The pool was filled with water to a depth of 30 cm at a temperature of (25 ± 2) °C, and was surrounded on all sides by white curtains containing various prominent visual cues. All rats were trained to locate a black underwater escape platform (14 cm in diameter) positioned at the midpoint of the target quadrant and submerged ~ 1.0 cm below the water surface. The swimming activity of each rat was monitored *via* an overhead camera. A video-tracking system (Ethovision 3.0, Noldus Information Technology,

Wageningen, The Netherlands) was used to collect movement information (latency, swim path, distance, and speed). On each training day, a trial was initiated by placing each rat in the water facing the pool wall in one of the four quadrants and allowing it to swim freely to the escape platform. When the rat found the platform, it was allowed to stay on it for 10 s. If it did not find the platform within 120 s, the rat was guided gently to it. And then the rat was placed back in the home cage for 20 s before the next trial. Each animal was trained four times per day for 5 consecutive days. Twenty-four hours after completing the hidden platform trials, each animal was given a 120-s probe trial to evaluate the retention of the learned task. During the probe test, the platform was removed and the searching behavior in the target quadrant (where the platform was located during hidden training) was measured. After the probe test, the visual and motor ability of rats was assessed using a visible platform test. The time and the swimming speed of rats arriving at the target platform were recorded.

Real-Time PCR

After the behavioral tests, the hippocampi were rapidly removed under general anesthesia with urethane. The hippocampus from one side was used for measurements of STAT3 (signal transducers and activators of transcription) and caspase3 gene expression by real-time PCR. The total RNA in the hippocampus was isolated with TRIzol (15596-026, Invitrogen, New York, NY). The RNA concentration was determined using a biophotometer (Shanghai Scientific, Shanghai, China). Total RNA (1 μ g) was reverse-transcribed with the PrimeScriptTM RT reagent kit (Takara Biotechnology, Dalian, China). Quantitative real-time PCR amplification was performed using the SYBR Premix Ex TaqTM II PCR kit (TaKaRa Biotechnology, Dalian, China). PCR reactions and data analysis were performed using Mx3005P QPCR Systems (Agilent Stratagene, Santa Clara, CA). The relative quantity of mRNA was calculated from a GAPDH standard curve. The sequences of the primers were as follows: caspase-3, sense 5'-GAGACAGACAGTGA GAACTGACGATG-3', antisense 5'-GGCGCAAAGTGA CTGGATGA-3'; STAT3, sense 5'-AGAGCCAGGAG CACCCTGAA-3', antisense 5'-GGTCAATGGTATTGCT GCAGGTC-3'; GAPDH, sense 5'-GGCACAGTCAAGGC TGAGAAT-3', antisense 5'-ATGGTGGTGAAGACGCCA GTA-3'. Total hippocampal RNA was extracted using TRIzol according to the manufacturer's instructions.

Western Blot

The hippocampus from the other side was used for measuring STAT3 and caspase3 protein expression by western

blot. The hippocampus was homogenized in tissue protein extraction reagent (Boster, Inc, Wuhan, China) supplemented with complete protease and phosphatase inhibitor (Boster, Inc, Wuhan, China). The homogenates were centrifuged (30 min, 15,000 rpm, 4 °C), and protein concentrations were measured using a BCA kit (Boster, Inc, Wuhan, China). A total of 50 µg of protein from each sample was used. Sample proteins were separated on 12% SDS-polyacrylamide gels. After electrophoresis, the proteins were transferred onto 0.45 µm PVDF membranes (Solarbio, Inc, Beijing, China) and nonspecific binding was blocked with 5% BSA (Solarbio, Inc, Beijing, China) in Tris-buffered saline containing 0.05% Tween-20 (TBST). The membranes were incubated with a primary antibody overnight at 4 °C, followed by a secondary antibody for 2 h at 4 °C. The primary antibodies used were as follows: rabbit polyclonal cleaved caspase-3 (Asp 175) antibody (Cell Signaling Technology #9661, dilution 1:1000), rabbit polyclonal caspase-3 antibody (Cell Signaling Technology #9662, dilution 1:1000), rabbit polyclonal anti-STAT3 (phospho S727) antibody (Abcam ab30647, dilution 1:750), and rabbit monoclonal anti-STAT3 antibody (Abcam ab68153, dilution 1:1500). The secondary antibody was anti-rabbit IgG HRP (ZSGB-BIO Inc. Beijing, China, dilution 1:100,000). After rinsing with TBST, the immunocomplexes were visualized by chemiluminescence using ECL (Beyotime, Inc. Shanghai, China). The film signals were digitally scanned with a Fluor Chem Scanner (ProteinSimple) and quantified with Alpha View SA software. β -actin (PR-0255, ZSGB-BIO Inc. Beijing, China, dilution 1:500) was used as an internal control for sample loading, and each blot was normalized to its corresponding β -actin value.

Data Analysis

All values are expressed as mean \pm SEM. The data from hidden-platform test were assessed by two-repeated measures analysis of variance (ANOVA) with LSD post hoc analysis for multiple comparisons, and the other data were analyzed using one-way ANOVA. The significance level was defined as $P < 0.05$, and all tests were performed using SPSS version 18.

Results

$A\beta_{1-42}$ and $A\beta_{31-35}$ Almost Equally Impaired Spatial Learning and Memory in Rats

The ability of rats to acquire and maintain spatial information was first examined using the Morris water-maze. We found that pretreatment with $A\beta_{1-42}$ and $A\beta_{31-35}$

almost equally impaired spatial learning and memory. In hidden-platform tests (Fig. 1A), the average escape latencies in the control group ($n = 20$) were 94.8 ± 3.0 , 44.4 ± 1.9 , 24.1 ± 1.5 , 19.8 ± 0.8 , and 18.0 ± 1.1 s on training days 1–5. Bilateral intra-hippocampal injection of 2.0 nmol $A\beta_{1-42}$ or $A\beta_{31-35}$ significantly increased the average escape latencies from the second training day ($P < 0.01$), being 81.4 ± 4.3 , 45.0 ± 3.9 , 34.1 ± 2.1 , and 28.7 ± 1.8 s in the $A\beta_{1-42}$ group ($n = 10$), and 76.2 ± 2.8 , 42.2 ± 2.7 , 30.65 ± 2.1 , and 26.8 ± 1.4 s in the $A\beta_{31-35}$ group ($n = 20$). There was no statistical difference between the $A\beta_{31-35}$ and $A\beta_{1-42}$ group. In probe trials (Fig. 1B), the percentage swimming time elapsed in the target quadrant was $49.1 \pm 1.1\%$ in the control group, and this decreased to $35.2 \pm 1.8\%$ ($P < 0.01$) in the 2 nmol $A\beta_{1-42}$ group and to $38.4 \pm 1.4\%$ ($P < 0.01$) in the 2 nmol $A\beta_{31-35}$ group. However, the reversed sequence of $A\beta_{31-35}$, $A\beta_{35-31}$, did not affect these behaviors. The mean escape latency in the $A\beta_{35-31}$ group ($n = 10$) was 94.2 ± 5.3 , 43.4 ± 4.0 , 27.5 ± 2.6 , 23.3 ± 2.1 , and 19.8 ± 1.4 s on training days 1–5, and the percentage swimming time was $47.2 \pm 1.7\%$, without any significant differences compared with the control group ($P > 0.05$).

We then investigated the dose-response for higher concentrations of $A\beta_{31-35}$ (Fig. 1C, D). In the hidden-platform tests (Fig. 1C), the mean escape latency in the 20 nmol $A\beta_{31-35}$ group ($n = 10$) was longer than in the 2 nmol $A\beta_{31-35}$ group on days 2–5, being 90.9 ± 4.6 ($P < 0.01$), 68.6 ± 4.8 ($P < 0.01$), 49.7 ± 1.9 ($P < 0.01$), and 42.8 ± 2.2 s ($P < 0.01$). The 10 nmol $A\beta_{31-35}$ group ($n = 10$) also had a higher mean escape latency on training day 5 (33.2 ± 1.7 s) than the 2 nmol $A\beta_{31-35}$ group ($P < 0.01$). Compared with the 10 nmol $A\beta_{31-35}$ group, the mean escape latency in the 20 nmol $A\beta_{31-35}$ group was also higher on training days 4 ($P < 0.05$) and 5 ($P < 0.01$). Similarly, probe tests (Fig. 1D) showed that the percentage swimming time ($30.6 \pm 2.1\%$) in the 20 nmol $A\beta_{31-35}$ group was lower than in the 2 nmol $A\beta_{31-35}$ group ($38.4 \pm 1.4\%$; $P < 0.01$). Representative swimming tracks in probe trials on day 6 are shown in Fig. 1E.

HNG Protected Against $A\beta_{31-35}$ -Induced Impairments of Spatial Learning and Memory

To investigate whether HNG protects against $A\beta_{31-35}$ -induced cognitive impairment, we first examined the role of HNG alone on spatial learning and memory, and found that it had no effect (Fig. 2A, B). Compared to the control group, the mean escape latency and the percentage swimming time in the target quadrant did not change in the HNG alone group ($n = 10$, $P > 0.05$). Further, we investigated the effects of HNG on $A\beta_{31-35}$ -induced deficits in spatial learning and memory and found that the mean escape

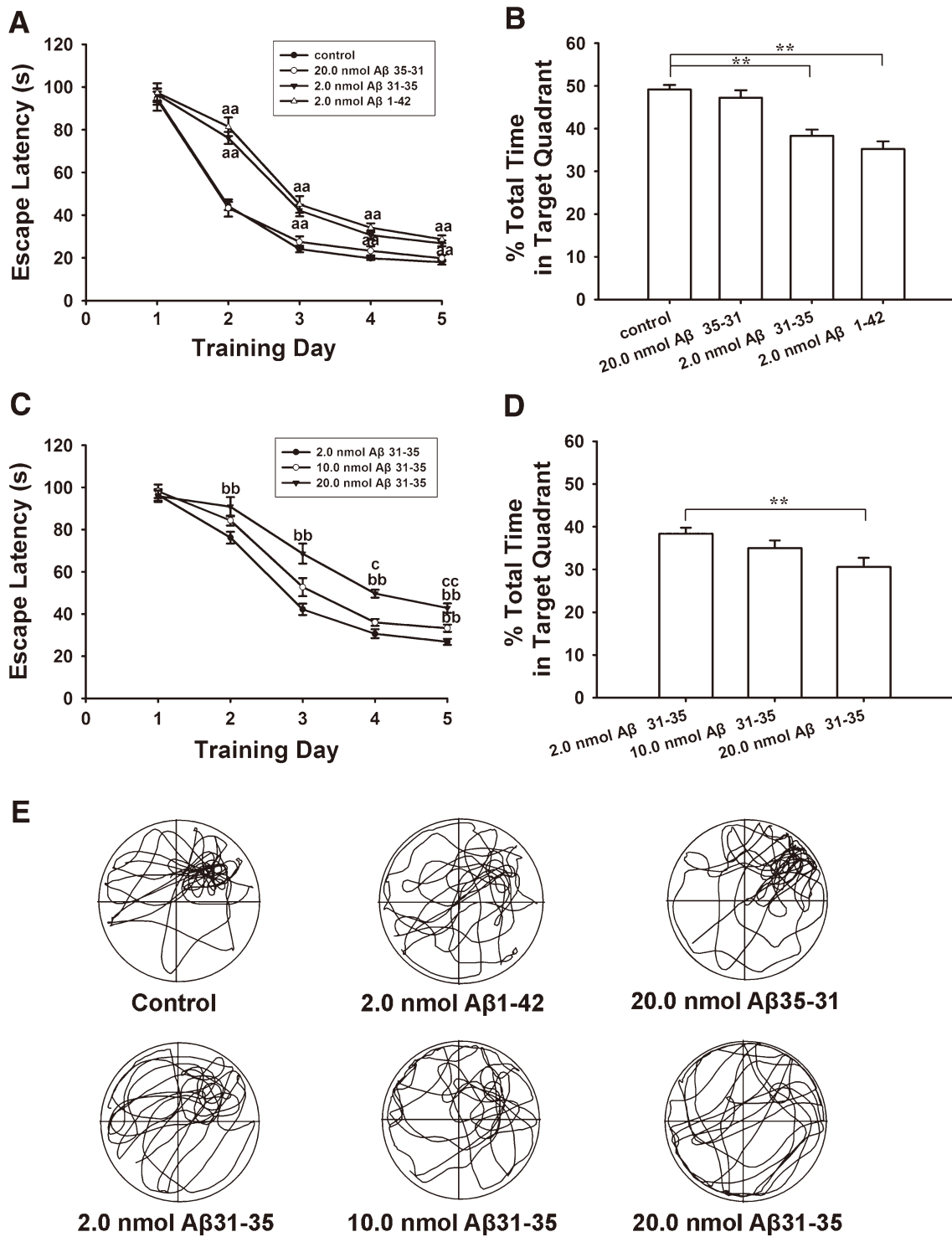


Fig. 1 Intra-hippocampal injection of A β ₁₋₄₂ and A β ₃₁₋₃₅, but not A β ₃₅₋₃₁, impaired spatial learning and memory in rats. **A, B**, Plots and histograms comparing the effects of 2 nmol of the different A β fragments on escape latency and percentage swimming time in the target quadrant. A β ₁₋₄₂ and A β ₃₁₋₃₅ almost equally increased the escape latency on training days 2–5 (^{aa}*P* < 0.01 compared with

control group). **C, D**, Plots and histograms showing that A β ₃₁₋₃₅ dose-dependently suppressed learning and memory (^{bb}*P* < 0.01 compared with 2.0 nmol A β ₃₁₋₃₅ group; ^c*P* < 0.05, ^{cc}*P* < 0.01 compared with 10.0 nmol A β ₃₁₋₃₅ group; ^{**}*P* < 0.01). Each point and column represents the mean \pm SEM. **E**, Representative swimming tracks in probe trials on day 6.

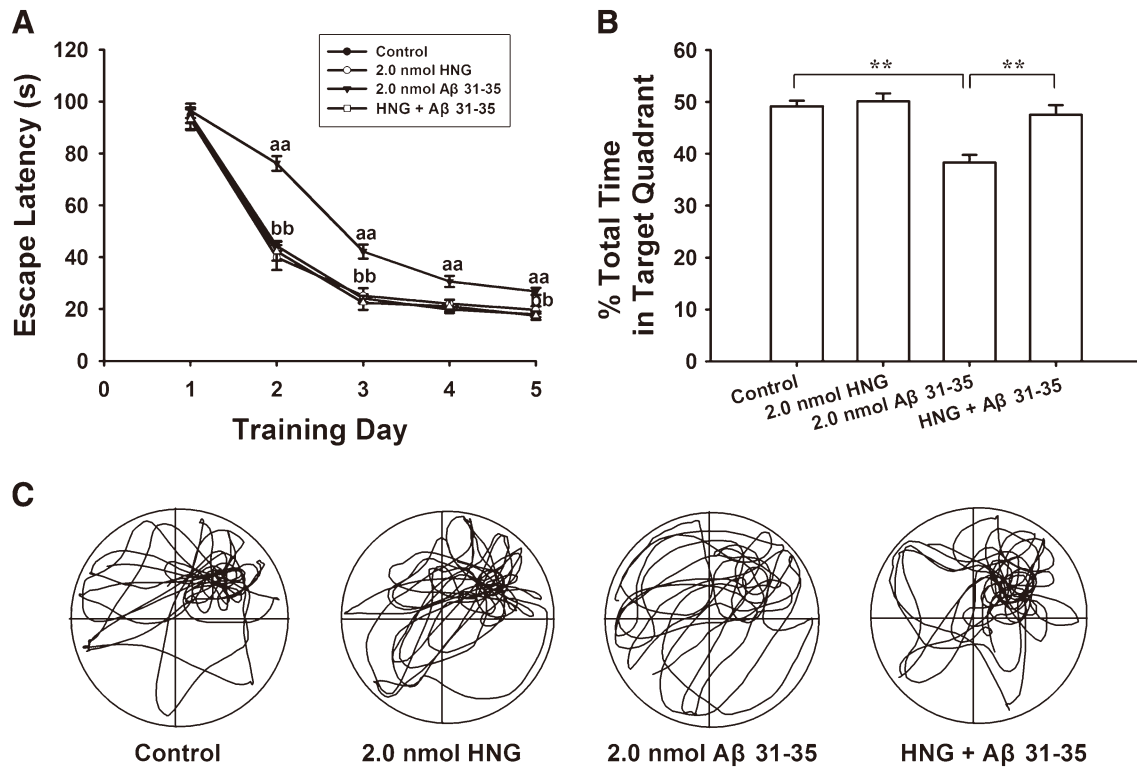


Fig. 2 HNG prevented A β_{31-35} -induced deficits in spatial learning and memory in rats. **A**, Average escape latency for finding the hidden underwater platform (^{aa} $P < 0.01$ compared with control group; ^{bb} $P < 0.01$ compared with 2.0 nmol A β_{31-35} group). **B**, Percentage of swimming time in the previous target quadrant. HNG alone did not

affect the spatial cognitive function but prevented A β_{31-35} -induced memory deficits ($**P < 0.01$). Each point or column represents the mean \pm SEM. **C**, Representative swimming tracks in probe trials on day 6.

latency decreased to 93.1 ± 4.0 , 42.3 ± 3.6 , 22.4 ± 2.7 , 21.0 ± 2.5 , and 17.5 ± 1.6 s in the HNG + A β_{31-35} group ($n = 10$) on training days 1–5, shorter ($P < 0.01$) than the mean escape latency in the A β_{31-35} alone group at all time points except training day 1 ($P > 0.05$). In addition, the swimming time in the target quadrant after removing the platform increased, from $38.4 \pm 1.4\%$ in the A β_{31-35} alone group to $47.5 \pm 1.9\%$ in the HNG + A β_{31-35} group ($P < 0.01$). Typical swim trajectories in probe tests are shown in Fig. 2C. These results indicate that HNG pretreatment prevents A β_{31-35} -induced impairments in spatial learning and memory in rats.

Neither Vision Nor the Motor Ability of Rats Were Affected by Any of the Drugs Used

To exclude the influence of vision and motor ability on spatial cognition, we measured the average escape latency in the visible platform condition and compared the swimming speeds during all training days. There was no difference in the escape latency among all groups ($P > 0.05$) in the visible platform test, with an average of ~ 15.4 s spent reaching the visible platform. In addition, there was

no statistical difference ($P > 0.05$) in swimming speeds among all groups during the 5 consecutive days of learning acquisition, the average being ~ 20.7 cm/s.

Tyrosine Kinase Inhibitor Genistein Attenuated the Protective Effects of HNG

To determine whether the tyrosine kinase pathway is involved in the neuroprotective action of HNG, we used the specific tyrosine kinase inhibitor genistein in behavioral experiments. Injection of genistein alone ($n = 10$) did not change the escape latency and the percentage swimming time ($P > 0.05$). However, genistein almost completely abolished the protective action of HNG against A β_{31-35} . In the genistein + HNG + A β_{31-35} group ($n = 10$), the average escape latency returned to 65.5 ± 5.8 ($P < 0.01$), 48.8 ± 5.6 ($P < 0.01$), 37.2 ± 3.0 ($P < 0.05$), and 28.6 ± 2.5 s ($P < 0.01$) on training days 2–5, significantly greater than the corresponding values in the HNG + A β_{31-35} group (Fig. 3A). The percentage swimming time also decreased to $33.3 \pm 2.0\%$ from $47.5 \pm 1.9\%$ in the HNG + A β_{31-35} group ($P < 0.01$, Fig. 3B). These results indicate that tyrosine kinase receptors mediate the

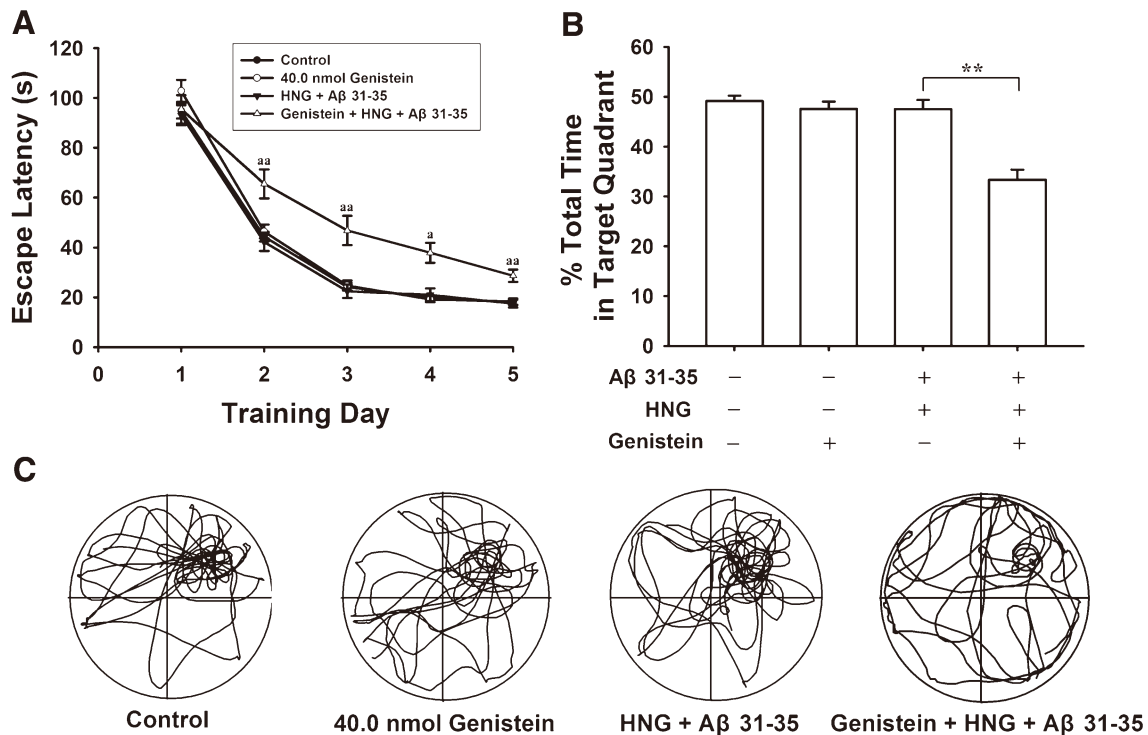


Fig. 3 Genistein abolished the protective effects of HNG against A β_{31-35} -induced impairment of spatial memory in rats. **A**, Escape latency for finding the hidden platform over five consecutive training days (^a $P < 0.05$, ^{aa} $P < 0.01$ compared with HNG + A β_{31-35} group).

B, Percentage of swimming time in the previous target quadrant (^{**} $P < 0.01$). Each point and column represents the mean \pm SEM. **C**, Representative swimming tracks in probe trials on day 6.

protective effect of HNG against A β_{31-35} -induced spatial cognitive damage.

A β_{31-35} and HNG Differentially Modulated the Expression Levels of Caspase-3 and STAT3

We further used real-time PCR and western blotting to assess the mRNA and protein expression levels of hippocampal caspase-3 and STAT3, two factors critically involved in neuronal apoptosis and cell survival in AD. Compared with the control group (0.99 ± 0.02 , $n = 7$), the level of caspase-3 mRNA increased ($P < 0.01$) in the A β_{31-35} alone group (1.25 ± 0.06 , $n = 7$), and decreased ($P < 0.01$) in the HNG alone group (0.69 ± 0.05 , $n = 7$; Fig. 4A). Even in the presence of A β_{31-35} , the caspase-3 mRNA still remained relatively lower in the HNG + A β_{31-35} group (0.64 ± 0.05 , $n = 7$), lower than in the A β_{31-35} alone group (1.25 ± 0.06 , $P < 0.01$). On the contrary, the level of STAT3 mRNA (Fig. 4B) clearly decreased in the A β_{31-35} alone group (0.74 ± 0.05 , $n = 7$, $P < 0.01$) and increased in the HNG alone group (1.23 ± 0.07 , $n = 7$, $P < 0.01$), compared with the control group (0.99 ± 0.03 , $n = 7$). Similarly, the A β_{31-35} -induced STAT3 mRNA decrease was effectively reversed by HNG, from 0.74 ± 0.05 in the A β_{31-35} alone group to 1.11 ± 0.05 in the HNG + A β_{31-35} group ($P < 0.01$). Moreover, the

modulatory effects of HNG on caspase-3 and STAT3 were totally antagonized by pretreatment with genistein, a tyrosine kinase inhibitor. The levels of caspase-3 and STAT3 mRNA in the genistein + HNG + A β_{31-35} group returned to 1.28 ± 0.05 and 0.65 ± 0.06 , respectively, different from the values in the HNG + A β_{31-35} group ($P < 0.01$).

We found similar results in western blotting experiments. Pretreatment with HNG significantly suppressed the A β_{31-35} -induced activation of cleaved caspase-3 and the down-regulation of phosphorylated STAT3 (Ser 727) in the hippocampus (Fig. 5). However, the protein level of cleaved caspase-3 (Fig. 5B) increased ($P < 0.05$), while the phosphorylated STAT3 (Ser 727) (Fig. 5D) decreased ($P < 0.05$) in the A β_{31-35} alone group ($n = 6$). In the HNG + A β_{31-35} group ($n = 7$), HNG pretreatment effectively reversed the A β_{31-35} -induced changes in protein level ($P < 0.05$ for both). Furthermore, the modulatory effects of HNG on cleaved caspase-3 and STAT3 were all antagonized by genistein ($P < 0.05$).

Discussion

The neurotoxicity of A β , especially the soluble A β oligomer, has been reported *in vivo* and *in vitro* [13, 14]. A β_{1-42} and A β_{1-40} are natural pathogenic species in the human AD

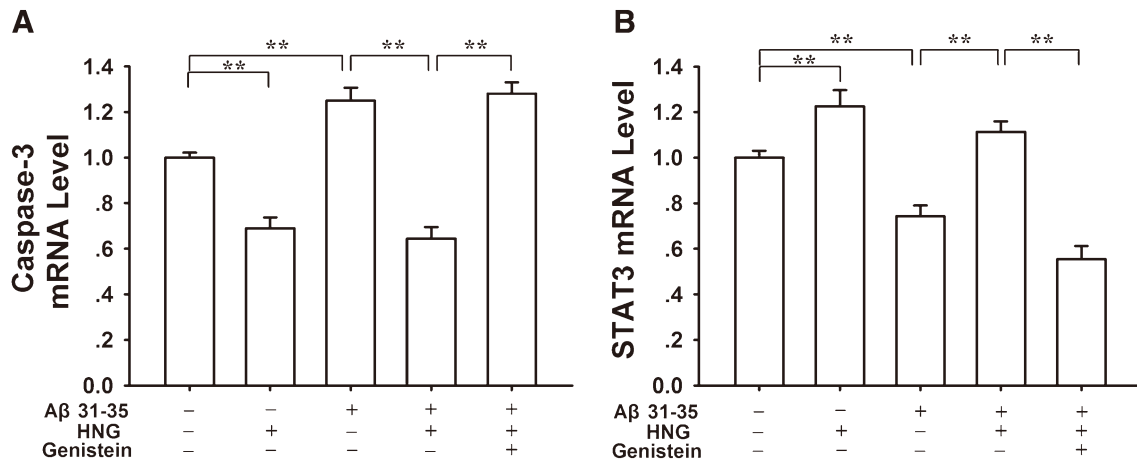


Fig. 4 Effects of A β_{31-35} and HNG on expression levels of caspase-3 and STAT3 mRNA in rat hippocampus. **A**, Histogram showing that the A β_{31-35} -induced increase in caspase-3 mRNA was suppressed by HNG, and this was blocked by genistein, a tyrosine kinase inhibitor.

B, Histogram showing that the A β_{31-35} -induced inhibition of STAT3 mRNA was reversed by HNG, and this was also blocked by genistein. Each column represents the mean \pm SEM (** $P < 0.01$).

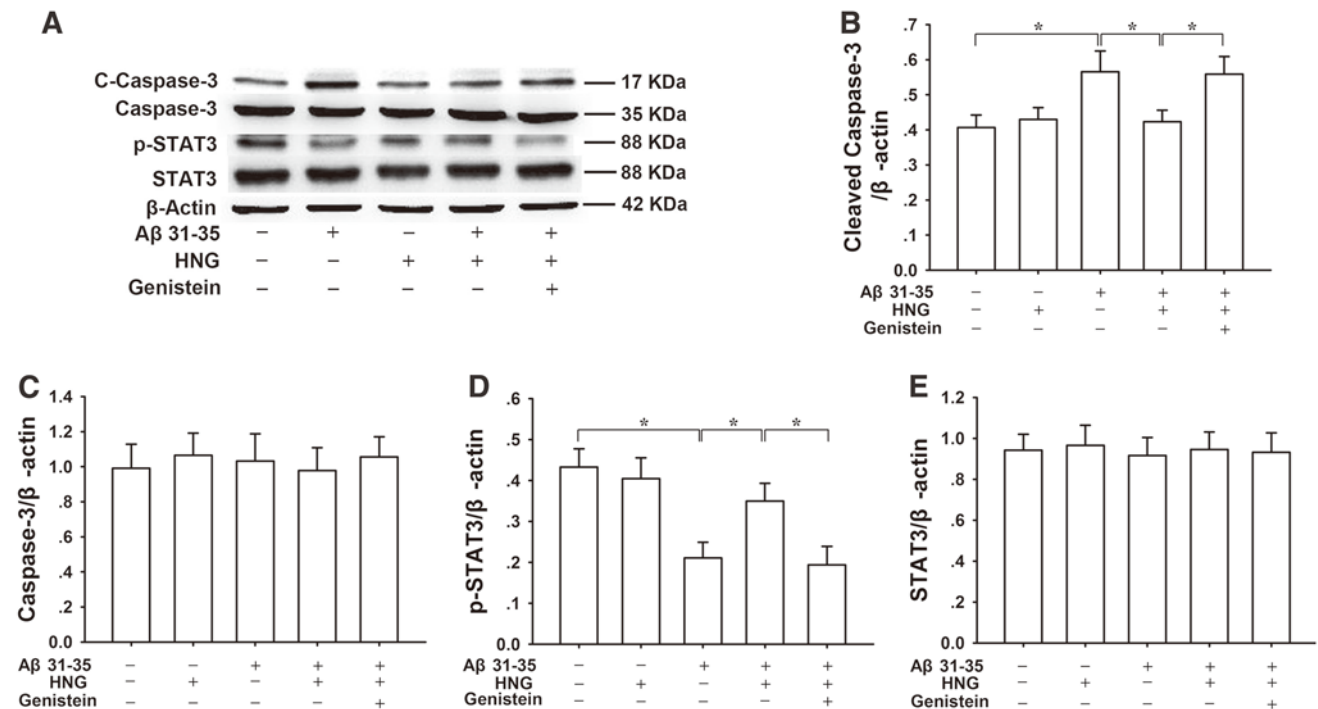


Fig. 5 Effects of A β_{31-35} and HNG on protein expression levels of caspase-3 and STAT3 in rat hippocampus. **A**, Representative western blots of cleaved caspase-3 (Asp 175), total caspase-3, pSTAT3 (Ser 727), and total STAT3. **B–E**, Quantitative analyses of western blots

for cleaved caspase-3 (**B**), total caspase-3 (**C**), phosphorylated STAT3 (Ser 727) (**D**), and total STAT3 (**E**). Each column represents the mean \pm SEM (* $P < 0.05$).

brain. However, the active center of the A β molecule was still uncertain, and stronger *in vivo* evidence was still needed. The 25–35 sequence of A β is thought to be the active center of the full-length A β molecule because its neurotoxicity is similar to that of natural A β [15]. In the present behavioral study, we further demonstrated that bilateral intrahippocampal injections of A β_{1-42} and A β_{31-35}

almost equally impaired the spatial learning and memory of rats, and A β_{31-35} dose-dependently increased the escape latency and decreased the percentage swimming time. Meanwhile, A β_{35-31} , a fragment with the same amino-acids as A β_{31-35} but in reversed sequence, had no effect on spatial memory. These *in vivo* results are consistent with our previous findings that A β_{31-35} induces cell death in

cultured cortical neurons [16], forms new ion channels in membrane patches [9], and modulates synaptic plasticity in the hippocampus [7, 17]. It has been reported that the most important amino-acids associated with oxidative stress and the neurotoxicity of A β are isoleucine-31, glycine-33, and methionine-35 [18, 19]. It is interesting that these key amino-acids are all included in the 31–35 fragment we used in the present study. Therefore, we suggest that the 31–35 sequence in the A β molecule is the shortest active center responsible for its neurotoxicity, not only in neuronal apoptosis and synapse failure but also in behavioral deficits. In view of the different locations of the 31–35 sequence in harmful A β and beneficial APP (amyloid precursor protein), clarification of the A β active center will contribute to the design and development of novel anti-A β drugs that specifically target the extracellular A β but not the transmembrane APP.

As a neuroprotective factor, HN was first found in certain regions of the AD brain where A β was relatively sparse [20]. It has been reported that HN increases the ATP levels in serum-deprived human lymphocytes, TE671 muscle cells, and SKN-MC neural cells [21]. It also inhibits apoptosis and reduces the oxidative stress induced by A β_{1-42} [22]. The highly selective effect of HN on cell death associated with AD indicates that it could be promising for AD therapy [23, 24]. HNG, an important HN analogue, is well known for its strong neuroprotective action against AD-related toxic insults *in vitro* [25] and *in vivo* [26]. Our previous study revealed that HNG effectively prevents the LTP impairment and [Ca²⁺]_i elevation induced by A β fragments [11]. In the present study, we further confirmed that intra-hippocampal injection of HNG protected against A β -induced deficits in spatial long-term memory in rats. Similarly, Tajima *et al.* recently reported that intracerebroventricular injection of HNG prevents A β -induced impairments in the short-term memory of mice in a Y maze test [27]. These results suggest that HNG is promising for future AD treatment.

In the present study, we also attempted to clarify the molecular mechanisms underlying the neuroprotective action of HNG against the spatial learning and memory impairments induced by A β . HN secreted from cells can bind to membrane receptors and activate pro-survival signaling pathways, including certain tyrosine kinases linked to STAT3 [28]. So, we used genistein to determine whether tyrosine kinases were involved in the neuroprotective effect of HNG. Genistein is a specific inhibitor of tyrosine-specific protein kinases and has been reported to be effective in suppressing the EGF-stimulated increase in phosphotyrosine level and the SOV-induced increase in [Ca²⁺]_i [29, 30]. Our results showed that the neuroprotective effects of HNG against A β were mostly blocked by genistein, indicating that they involve the activation of

certain tyrosine protein kinases. It is well known that caspase3 and STAT3 are principal molecules in the signaling cascades mediated by tyrosine kinase. Increasing evidence has shown that the neuronal apoptosis occurring in AD is closely associated with high levels of activated caspase [13, 31, 32], while A β exposure [33] activates caspase-3 and causes abnormal processing of the microtubule-associated protein tau in AD models [34, 35]. On the contrary, STAT3 plays important roles in many cellular activities including survival, proliferation, differentiation, and apoptosis [36]. Therefore, activation of STAT3 may be critical for the HN-mediated neuroprotection, while inactivation of STAT3 may be involved in the A β -induced behavioral deficits. Indeed, our results from real-time PCR and western blot clearly demonstrated that A β_{31-35} significantly up-regulated the expression levels of caspase-3 mRNA and cleaved caspase-3 protein. On the contrary, A β_{31-35} injection down-regulated the expression levels of STAT3 mRNA and phosphorylated STAT3 (Ser 727). This differential regulation of caspase-3 and STAT3 may partially account for the impairment of spatial learning and memory by A β_{31-35} . More importantly, pretreatment with HNG not only alleviated the A β_{31-35} -induced behavioral disorder, but also blocked A β -induced caspase3 activation and STAT3 suppression. These results strongly suggest that the activation of STAT3, as well as the suppression of caspase-3, are involved in the neuroprotective actions of HNG. Consistent with our *in vivo* study, Guo *et al.* [11] reported that HNG protects PC12 cells against A β_{25-35} -induced cytotoxicity by suppressing caspase-3 activity.

In conclusion, by comparing the *in vivo* effects of three A β fragments and investigating the molecular mechanisms of action of A β and HNG, we have provided further evidence that the 31–35 sequence in A β is the shortest active center responsible for the neurotoxicity of A β from molecule to behavior, and the neuroprotective action of HNG against A β is closely associated with the activation of tyrosine kinases and the subsequent differential modulation of STAT3 and caspase3. Therefore, our findings raise the possibility that HNG may be used as a potential therapeutic agent for the treatment of AD.

Acknowledgements This work was supported by the National Natural Science Foundation of China (31271201 and 31471080).

References

1. Tanzi RE, Bertram L. Alzheimer's disease: The latest suspect. *Nature* 2008, 454: 706–708.
2. Jellinger KA, Bancher C. Neuropathology of Alzheimer's disease: a critical update. *J Neural Transm Suppl* 1998, 54: 77–95.
3. Zetterberg H, Blennow K, Hansson E. Amyloid beta and APP as biomarkers for Alzheimer's disease. *Exp Gerontol* 2010, 45: 23–29.

4. Wisniewski T, Goni F. Immunotherapeutic approaches for Alzheimer's disease. *Neuron* 2015, 85: 1162–1176.
5. Shi Z, Lu C, Sun X, Wang Q, Chen S, Li Y, *et al.* Tong Luo Jiu Nao ameliorates Abeta1-40-induced cognitive impairment on adaptive behavior learning by modulating ERK/CaMKII/CREB signaling in the hippocampus. *BMC Complement Altern Med* 2015, 15: 584.
6. Kaur N, Dhiman M, Perez-Polo JR, Mantha AK. Ginkgolide B revamps neuroprotective role of apurinic/aprimidinic endonuclease 1 and mitochondrial oxidative phosphorylation against Abeta -induced neurotoxicity in human neuroblastoma cells. *J Neurosci Res* 2015, 93: 938–947.
7. Zhang JF, Qi JS, Qiao JT. Protein kinase C mediates amyloid beta-protein fragment 31–35-induced suppression of hippocampal late-phase long-term potentiation in vivo. *Neurobiol Learn Mem* 2009, 91: 226–234.
8. Misiti F, Sampaiolese B, Pezzotti M, Marini S, Coletta M, Ceccarelli L, *et al.* Abeta(31–35) peptide induce apoptosis in PC 12 cells: contrast with Abeta(25–35) peptide and examination of underlying mechanisms. *Neurochem Int* 2005, 46: 575–583.
9. Qi JS, Qiao JT. Amyloid beta-protein fragment 31–35 forms ion channels in membrane patches excised from rat hippocampal neurons. *Neuroscience* 2001, 105: 845–852.
10. Qi JS, Ye L, Qiao JT. Amyloid beta-protein fragment 31–35 suppresses delayed rectifying potassium channels in membrane patches excised from hippocampal neurons in rats. *Synapse* 2004, 51: 165–172.
11. Guo F, Jing W, Ma CG, Wu MN, Zhang JF, Li XY, *et al.* [Gly(14)]-humanin rescues long-term potentiation from amyloid beta protein-induced impairment in the rat hippocampal CA1 region in vivo. *Synapse* 2010, 64: 83–91.
12. Ye L, Qiao JT. Suppressive action produced by beta-amyloid peptide fragment 31–35 on long-term potentiation in rat hippocampus is N-methyl-D-aspartate receptor-independent: it's offset by (-)huperzine A. *Neurosci Lett* 1999, 275: 187–190.
13. Mattson MP. Pathways towards and away from Alzheimer's disease. *Nature* 2004, 430: 631–639.
14. Ferreira ST, Vieira MN, De Felice FG. Soluble protein oligomers as emerging toxins in Alzheimer's and other amyloid diseases. *IUBMB Life* 2007, 59: 332–345.
15. Pan YF, Chen XR, Wu MN, Ma CG, Qi JS. Arginine vasopressin prevents against Abeta(25–35)-induced impairment of spatial learning and memory in rats. *Horm Behav* 2010, 57: 448–454.
16. Yan XZ, Qiao JT, Dou Y, Qiao ZD. Beta-amyloid peptide fragment 31–35 induces apoptosis in cultured cortical neurons. *Neuroscience* 1999, 92: 177–184.
17. Cheng L, Yin WJ, Zhang JF, Qi JS. Amyloid beta-protein fragments 25–35 and 31–35 potentiate long-term depression in hippocampal CA1 region of rats in vivo. *Synapse* 2009, 63: 206–214.
18. Kanski J, Aksenova M, Schoneich C, Butterfield DA. Substitution of isoleucine-31 by helical-breaking proline abolishes oxidative stress and neurotoxic properties of Alzheimer's amyloid beta-peptide. *Free Radic Biol Med* 2002, 32: 1205–1211.
19. Kanski J, Varadarajan S, Aksenova M, Butterfield DA. Role of glycine-33 and methionine-35 in Alzheimer's amyloid beta-peptide 1–42-associated oxidative stress and neurotoxicity. *Biochim Biophys Acta* 2002, 1586: 190–198.
20. Tajima H, Niikura T, Hashimoto Y, Ito Y, Kita Y, Terashita K, *et al.* Evidence for in vivo production of Humanin peptide, a neuroprotective factor against Alzheimer's disease-related insults. *Neurosci Lett* 2002, 324: 227–231.
21. Kariya S, Hirano M, Furiya Y, Ueno S. Effect of humanin on decreased ATP levels of human lymphocytes harboring A3243G mutant mitochondrial DNA. *Neuropeptides* 2005, 39: 97–101.
22. Chai GS, Duan DX, Ma RH, Shen JY, Li HL, Ma ZW, *et al.* Humanin attenuates Alzheimer-like cognitive deficits and pathological changes induced by amyloid beta-peptide in rats. *Neurosci Bull* 2014, 30: 923–935.
23. Niikura T, Chiba T, Aiso S, Matsuoka M, Nishimoto I. Humanin: after the discovery. *Mol Neurobiol* 2004, 30: 327–340.
24. Nishimoto I, Matsuoka M, Niikura T. Unravelling the role of Humanin. *Trends Mol Med* 2004, 10: 102–105.
25. Hashimoto Y, Niikura T, Tajima H, Yasukawa T, Sudo H, Ito Y, *et al.* A rescue factor abolishing neuronal cell death by a wide spectrum of familial Alzheimer's disease genes and Abeta. *Proc Natl Acad Sci U S A* 2001, 98: 6336–6341.
26. Miao J, Zhang W, Yin R, Liu R, Su C, Lei G, *et al.* S14G-Humanin ameliorates Abeta25–35-induced behavioral deficits by reducing neuroinflammatory responses and apoptosis in mice. *Neuropeptides* 2008, 42: 557–567.
27. Tajima H, Kawasumi M, Chiba T, Yamada M, Yamashita K, Nawa M, *et al.* A humanin derivative, S14G-HN, prevents amyloid-beta-induced memory impairment in mice. *J Neurosci Res* 2005, 79: 714–723.
28. Hashimoto Y, Suzuki H, Aiso S, Niikura T, Nishimoto I, Matsuoka M. Involvement of tyrosine kinases and STAT3 in Humanin-mediated neuroprotection. *Life Sci* 2005, 77: 3092–3104.
29. Russo M, Russo GL, Daglia M, Kasi PD, Ravi S, Nabavi SF, *et al.* Understanding genistein in cancer: The “good” and the “bad” effects: A review. *Food Chem* 2016, 196: 589–600.
30. Akiyama T, Ishide J, Nakagawa S, Ogaara H, Watanabe S, Itoh N. Genistein, a Specific Inhibitor of Tyrosine-specific Protein Kinases. *The Journal of Biological Chemistry* 1987, 262: 5592–5595.
31. Eckert A, Keil U, Marques CA, Bonert A, Frey C, Schussel K, *et al.* Mitochondrial dysfunction, apoptotic cell death, and Alzheimer's disease. *Biochem Pharmacol* 2003, 66: 1627–1634.
32. Mattson MP. Cellular actions of beta-amyloid precursor protein and its soluble and fibrillogenic derivatives. *Physiol Rev* 1997, 77: 1081–1132.
33. Jo J, Whitcomb DJ, Olsen KM, Kerrigan TL, Lo SC, Bru-Mercier G, *et al.* Abeta(1–42) inhibition of LTP is mediated by a signaling pathway involving caspase-3, Akt1 and GSK-3beta. *Nat Neurosci* 2011, 14: 545–547.
34. Chung CW, Song YH, Kim IK, Yoon WJ, Ryu BR, Jo DG, *et al.* Proapoptotic effects of tau cleavage product generated by caspase-3. *Neurobiol Dis* 2001, 8: 162–172.
35. Garwood CJ, Pooler AM, Atherton J, Hanger DP, Noble W. Astrocytes are important mediators of Abeta-induced neurotoxicity and tau phosphorylation in primary culture. *Cell Death Dis* 2011, 2: e167. doi:10.1038/cddis.2011.50
36. Kuchipudi SV. The Complex Role of STAT3 in Viral Infections. *J Immunol Res* 2015, 2015: 272359. doi:10.1155/2015/272359